CERN-TH/97-3
hep-ph/9701375

arXiv:hep-ph/9701375v1 24 Jan 1997

# Two-Loop Anomalous Dimension of the Chromo-Magnetic Moment of a Heavy Quark

G. Amorós*, M. Beneke and M. Neubert
*Theory Division, CERN, CH-1211 Geneva 23, Switzerland*

**Abstract**

We find that the anomalous dimension (in the $\overline{\rm MS}$ scheme) of the chromo-magnetic operator $g_s\bar{h}_v\sigma_{\mu\nu}G^{\mu\nu}h_v$ in the heavy-quark effective theory is

$$\gamma_{\rm mag} = \frac{C_A\alpha_s}{2\pi}\left[1+\left(\frac{17}{18}\,C_A-\frac{13}{18}\,T_F\,n_f\right)\frac{\alpha_s}{\pi}+O(\alpha_s^2)\right],$$

generalizing the one-loop expression known previously. To derive the two-loop result, we use the reparametrization invariance and the virial theorem. After performing infrared subtractions, all two-loop integrals are of propagator type and are evaluated by a recurrence relation for tensor integrals.

(Submitted to Physics Letters B)

CERN-TH/97-3
January 1997

*On leave from: Departament de Física Teòrica, Universitat de València, Spain

# 1 Introduction

The heavy-quark effective theory (HQET) is a convenient tool to describe the physics of hadrons containing a heavy quark [1]. It provides a systematic expansion around the limit $m_Q \to \infty$, in which new symmetries of the strong interactions arise, relating the long-distance properties of many observables to a small number of hadronic matrix elements. The effective Lagrangian of the HQET is [2]–[4]

$$\mathcal{L}_{\rm eff} = \bar h_v\, iv\cdot D\, h_v + \frac{C_{\rm kin}}{2m_Q}\,\bar h_v (iD)^2 h_v + \frac{C_{\rm mag}\, g_s}{4m_Q}\,\bar h_v \sigma_{\mu\nu} G^{\mu\nu} h_v + O(1/m_Q^2)\,, \tag{1}$$

where $g_s G^{\mu\nu} = i[D^\mu, D^\nu]$ is the gluon field-strength tensor, and $h_v$ the velocity-dependent field describing a heavy quark inside a hadron moving with velocity $v$. This field is subject to the constraint $\not v\, h_v = h_v$. The leading term in the effective Lagrangian, which gives rise to the Feynman rules of the HQET, is invariant under a global $SU(2n_h)$ spin–flavour symmetry group, where $n_h$ is the number of heavy-quark flavours. This symmetry is broken by the higher-dimensional operators arising at order $1/m_Q$. The first operator corresponds to the kinetic energy of the heavy quark inside the hadron, and the second operator describes the magnetic interaction of the heavy-quark spin with the gluon field. The coefficients $C_{\rm kin}$ and $C_{\rm mag}$ result from short-distance effects and, in general, depend on the scale at which the operators are renormalized.

Hadronic matrix elements of the higher-dimensional operators in (1) play a significant role in many applications of the HQET. It is therefore important to study the properties of these operators, in particular under renormalization. The reparametrization invariance of the HQET (an invariance under infinitesimal changes of the velocity) implies that, in regularization schemes with a dimensionless regulator, the kinetic operator is not renormalized, i.e. $C_{\rm kin} = 1$ to all orders in perturbation theory [5]. (In regularization schemes with a dimensionful regulator, the kinetic operator mixes with lower-dimensional operators [6, 7].) The renormalization of the chromo-magnetic operator at the one-loop order is known for some time [3, 4]. It is governed by the anomalous dimension, defined as

$$\gamma_{\rm mag} = Z_{\rm mag}\,\frac{{\rm d}Z_{\rm mag}^{-1}}{{\rm d}\ln\mu} = 2\alpha_s\,\frac{\partial}{\partial\alpha_s}\,Z_{\rm mag}^{(1)}\,, \tag{2}$$

where $Z_{\rm mag}$ is the renormalization constant that relates the bare operator with the renormalized one, $O_{\rm mag} = Z_{\rm mag}\, O_{\rm mag}^{\rm bare}$. The last relation is valid in dimensional regularization with a MS-like subtraction scheme, such as $\overline{\rm MS}$ [8], and follows from the requirement that the anomalous dimension be finite as $\epsilon = (4-d)/2 \to 0$ [9]. $Z_{\rm mag}^{(1)}$ denotes the coefficient of the $1/\epsilon$ pole in $Z_{\rm mag}$. At the one-loop order, $\gamma_{\rm mag} = C_A\alpha_s/2\pi$ [3, 4]. In this paper, we calculate the anomalous dimension to two-loop order. This completes the renormalization of the HQET Lagrangian at order $1/m_Q$, and to next-to-leading order in $\alpha_s$.

A direct calculation of the renormalization factor $Z_{\rm mag}$ at order $\alpha_s^2$ would require the evaluation of a large number of two-loop diagrams. The equivalent calculation for the chromo-magnetic operator of a light quark has been performed in Ref. [10]. For heavy

quarks, we follow a different strategy, which exploits the symmetries of the HQET. Instead of the chromo-magnetic operator itself, we study the renormalization of the two operators

$$O_1^{\mu\nu} = g_s \bar{h}_v \Gamma \, iG^{\mu\nu} h_v \,, \qquad O_2^{\mu\nu} = v^\mu v_\rho O_1^{\rho\nu} - v^\nu v_\rho O_1^{\rho\mu} \,. \tag{3}$$

For the special choice $\Gamma = -i\sigma_{\mu\nu}$, the first operator reduces to the chromo-magnetic operator, while the second one vanishes. Because the Feynman rules of the HQET do not involve $\gamma$ matrices, the Dirac structure of $\Gamma$ is not altered by radiative corrections, and it is of advantage to treat it as a general matrix. Then the operators $O_1^{\mu\nu}$ and $O_2^{\mu\nu}$ form a basis of physical (class-1) operators, i.e. operators that do not vanish by the equations of motion. The mixing of these operators under renormalization is such that [11]

$$O_1^{\mu\nu} = Z_1 \, O_{1,\mathrm{bare}}^{\mu\nu} + Z_2 \, O_{2,\mathrm{bare}}^{\mu\nu} \,, \qquad O_2^{\mu\nu} = (Z_1 + Z_2) \, O_{2,\mathrm{bare}}^{\mu\nu} \,. \tag{4}$$

In the rest frame of the heavy quark, the operator $O_2^{\mu\nu}$ contains only chromo-electric field components. The virial theorem of the HQET [12] relates this operator to the kinetic operator in (1). Since the kinetic operator is not renormalized, we have the exact relation $Z_1 + Z_2 = 1$, i.e. [11]

$$Z_{\mathrm{mag}} = Z_1 = 1 - Z_2 \,. \tag{5}$$

Below we calculate $Z_2$ to order $\alpha_s^2$, and then use (5) and (2) to obtain the two-loop anomalous dimension of the chromo-magnetic operator.

# 2 Two-loop Calculation

The particular structure of the operator $O_2^{\mu\nu}$ greatly facilitates the calculation. To obtain the factor $Z_2$ in (4) at order $\alpha_s^2$, we calculate the insertion of $O_1^{\mu\nu}$ into the amputated Green function with two heavy quarks and a (background-field) gluon to two-loop order, as well as the one-loop diagrams with counterterm insertions needed to subtract the subdivergences of the two-loop diagrams. However, we only need to evaluate those diagrams giving a contribution proportional to the tree-level matrix element of $O_2^{\mu\nu}$:

$$\langle O_2^{\mu\nu} \rangle = g_s t_a \Gamma \left[ v^\alpha (q^\mu v^\nu - q^\nu v^\mu) + v \cdot q \, (v^\mu g^{\alpha\nu} - v^\nu g^{\alpha\mu}) \right] \,, \tag{6}$$

where $v$ is the heavy-quark velocity, $t_a$ a colour matrix, $\alpha$ and $a$ the Lorentz and colour indices of the gluon, and $q$ the incoming gluon momentum. It suffices to trace in our calculation the terms proportional to $v^\alpha v^\nu q^\mu$, as no other operators yield this Lorentz structure. Then, taking into account the Feynman rules of the HQET, it is straightforward to derive the following selection rules:

1. If the external gluon is attached to the operator, the diagram is proportional to $g^{\mu\alpha}$ or $g^{\nu\alpha}$ and does not contribute to the structure $v^\alpha v^\nu q^\mu$.

2. If the external gluon is attached to a heavy-quark line, the diagram only depends on $v \cdot q$ and does not contribute to the desired structure. On the other hand, the external gluon must be connected to a heavy-quark line through other gluons (or through a light-fermion or ghost loop), otherwise one cannot get $v^\alpha$.

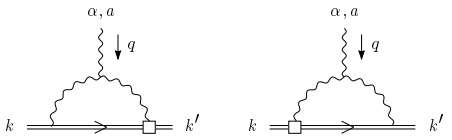


Figure 1: One-loop diagrams contributing to the calculation of the renormalization factor $Z_2$. The operator $O_1^{\mu\nu}$ is represented by a square.

3. The external gluon must be connected to the operator through other gluons (or through a light-fermion or ghost loop). If it is not, one cannot get $q^\mu$.

Accounting for these rules, only the two diagrams shown in Fig. 1 need to be calculated at the one-loop order. They give identical contributions. At the two-loop order, all diagrams that yield terms proportional to $v^\alpha v^\nu q^\mu$ can be generated by first drawing the two-loop diagrams that contribute to the heavy-quark two-point function with an insertion of $O_1^{\mu\nu}$, and then attaching an external gluon in all possible ways to one of the gluon, ghost or light-quark lines or vertices. This gives rise to the graphs shown in Fig. 2.

In evaluating the two-loop diagrams, we only need to keep terms linear in the gluon momentum $q$. Because the pole parts are polynomial in the external momenta, we can first take one derivative with respect to $q$ and then set $q = 0$ and $k = k'$, so that all integrals are of propagator type and depend on the single variable $\omega = v \cdot k = v \cdot k'$, where $k$ and $k'$ are the external momenta of the heavy quarks. However, this straightforward application of the method of infrared (IR) rearrangement [13] fails for some of the diagrams ($D_2$, $D_5$, $D_7$, $D_{13}$, $D_{15}$, $D_{18}$ and $D_{21}$), for which setting $q = 0$ after differentiation leads to IR divergences. In these cases, we apply a simple variant of the so-called $R^*$ operation [14], which compensates these IR poles by a recursive construction of counterterms for the IR divergent subgraphs. In our case, after accounting for UV and IR counterterms in all subgraphs, the overall counterterm is purely UV and gives rise to the desired contribution to the anomalous dimension.

To illustrate the procedure, consider a typical integral, which arises (as coefficient of $q^\mu$) in the calculation of $D_2$:

$$I = \int \mathrm{d}^d s \, \mathrm{d}^d t \, \frac{t^\beta t^\gamma}{(v \cdot s + \omega)(v \cdot t + \omega)(-s^2)[-(s+q)^2](-t^2)[-(t-s)^2]} \,. \tag{7}$$

For $q = 0$, this integral has an IR divergence when $s \to 0$. To construct the IR counterterm that compensates this singularity, we subtract and add the integral

$$I_{\mathrm{IR}} = \int \mathrm{d}^d s \, \frac{1}{(-s^2)[-(s+q)^2]} \int \mathrm{d}^d t \, \frac{t^\beta t^\gamma}{\omega \, (v \cdot t + \omega)(-t^2)^2} \,, \tag{8}$$

which is obtained by setting $s = 0$ whenever possible (i.e. by neglecting $s$ compared with $t$, and $v \cdot s$ compared with $\omega$). The two integrals $I$ and $I_{\mathrm{IR}}$ have the same behaviour for $s \to 0$; their difference is IR finite and can be evaluated for $q = 0$. In this case

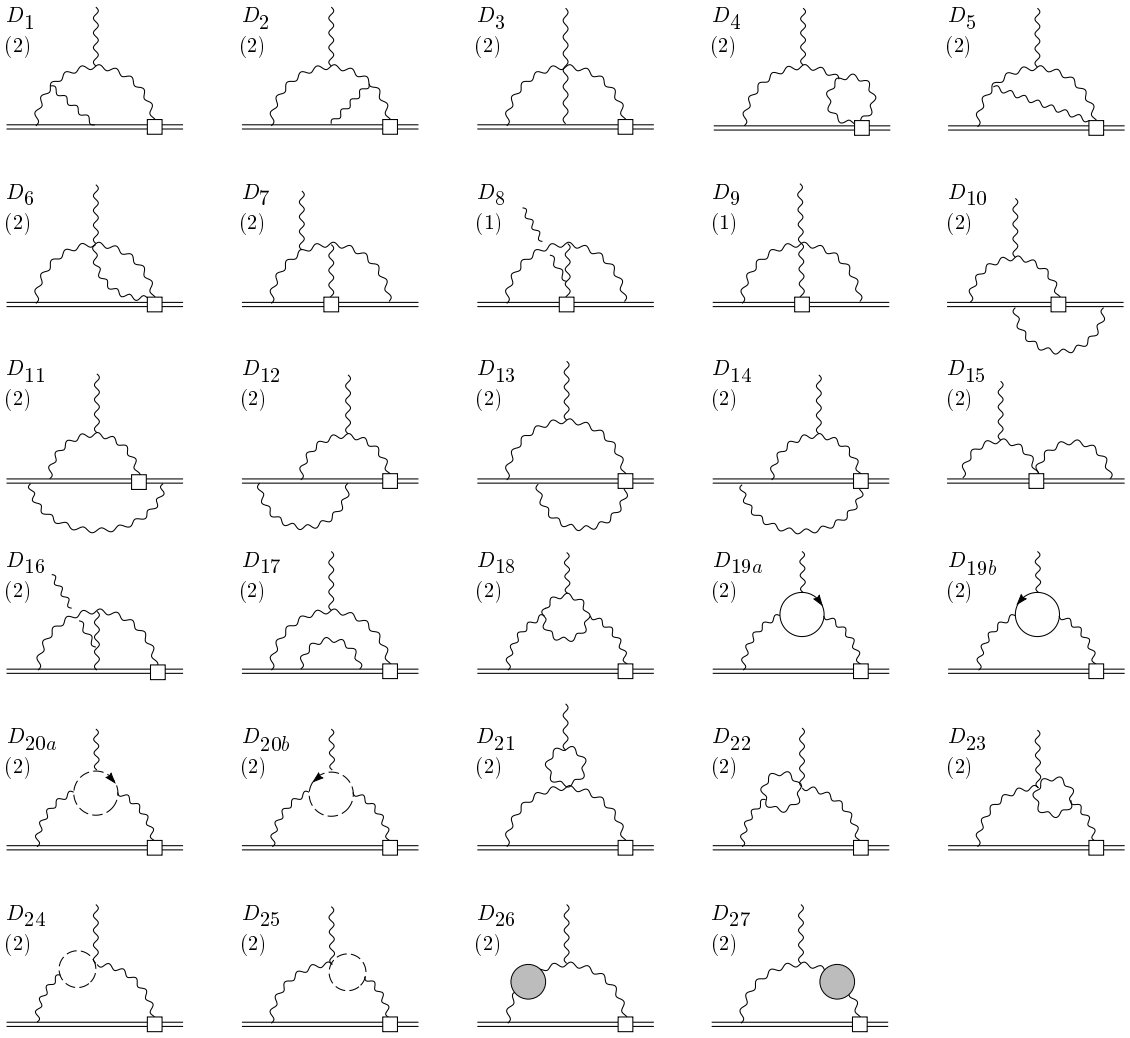


Figure 2: Two-loop diagrams contributing to the calculation of the renormalization factor $Z_2$. The notation (2) indicates that a mirror copy of the diagram is included implicitly. The shaded circles represent one-loop self-energy insertions.

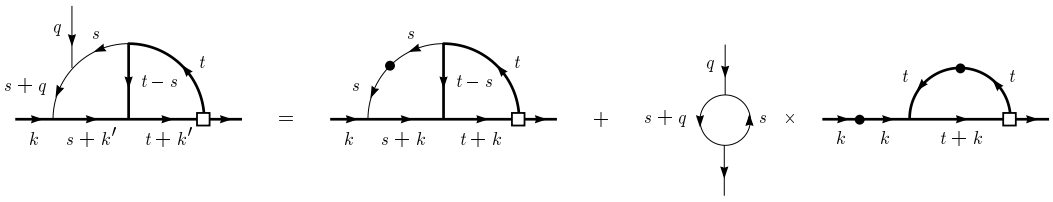


Figure 3: Schematic representation of the $R^*$ operation. Thick (thin) lines show propagators with a large (small) momentum flow. The black dots represent the original vertices.

$I_{\rm IR}$ becomes a tadpole integral and vanishes, so that $(I - I_{\rm IR})_{q=0}$ coincides with the original integral with $q$ set to zero. This integral can be calculated using the general algorithm described below. On dimensional grounds, it is proportional to $(-2\omega)^{-4\epsilon}$. The contribution $I_{\rm IR}$, which is necessary to subtract the IR subdivergence of the original integral $I$, factorizes into an IR counterterm (the $s$ integral) and the original diagram with the lines of the IR sensitive subgraph removed. This deletion of lines follows from the locality of IR divergences in momentum space. Because of this factorization, IR subtraction terms such as $I_{\rm IR}$ are proportional to $(-2\omega)^{-2\epsilon}(-q^2)^{-\epsilon}$. The construction just described is schematically shown in Fig. 3. It is necessary that exactly the same treatment is followed for the one-loop UV counterterms associated with a given diagram. Then the $1/\epsilon$ poles proportional to $\ln(-2\omega/\mu)$ and $\ln(-q^2/\mu^2)$ are cancelled for each diagram, and the final overall counterterm is local.

All integrals can be treated in the above manner. The remaining two-loop tensor integrals are of the general form

$$\begin{aligned}&\int \mathrm{d}^d s\, \mathrm{d}^d t\, \left(\frac{\omega}{v\cdot s+\omega}\right)^{\alpha_1} \left(\frac{\omega}{v\cdot t+\omega}\right)^{\alpha_2} \frac{s_{\mu_1}\dots s_{\mu_n} t^{\nu_1}\dots t^{\nu_m}}{(-s^2)^{\alpha_3}(-t^2)^{\alpha_4}[-(s-t)^2]^{\alpha_5}} \\ &\equiv -\pi^d(-2\omega)^{2(d-\alpha_3-\alpha_4-\alpha_5)+n+m}\, I^{\nu_1\dots\nu_m}_{\mu_1\dots\mu_n}(\{\alpha_i\})\,. \end{aligned} \tag{9}$$

The diagrams $D_{10}$ and $D_{12}$ can be brought into this form by multiplication with

$$1 = \frac{1}{\omega}\Big\{(v\cdot s+\omega)+(v\cdot t+\omega)-[v\cdot(s+t)+\omega]\Big\}\,. \tag{10}$$

A standard method is to reduce the tensor integrals to scalar two-loop integrals, which can be calculated in an algorithmic way [15]. However, since in our case we need integrals with up to five tensor indices, the reduction to scalar integrals would be rather involved. Therefore, we compute the tensor integrals directly. Using the method of integration by parts [16], we obtain the recurrence relation

$$\begin{aligned}&\Big[(d-\alpha_1-\alpha_3-2\alpha_5+n)+\alpha_3\,\mathbf{3}^+(\mathbf{4}^- - \mathbf{5}^-)+\alpha_1\,\mathbf{1}^+\mathbf{2}^-\Big]\; I^{\nu_1\dots\nu_m}_{\mu_1\dots\mu_n}(\{\alpha_i\}) \\ &\quad = \sum_{j=1}^{n} I^{\mu_j\nu_1\dots\nu_m}_{\mu_1\dots[\mu_j]\dots\mu_n}(\{\alpha_i\})\,, \end{aligned} \tag{11}$$

which allows us to express any two-loop integral in terms of degenerate integrals, which have $\alpha_2 = 0$, $\alpha_4 = 0$ or $\alpha_5 = 0$. Here $\mathbf{1}^+$ is an operator raising the index $\alpha_1$ by one unit etc., and $[\mu_j]$ means that this index is omitted. The degenerate integrals can be expressed in terms of products of one-loop tensor integrals, which are given by

$$\begin{aligned}\int \mathrm{d}^d s\, \left(\frac{\omega}{v\cdot s+\omega}\right)^{\beta} \frac{s^{\mu_1}\dots s^{\mu_n}}{(-s^2)^{\alpha}} &= i\pi^{d/2} I_n(\alpha,\beta)\,(-2\omega)^{d-2\alpha+n}\, K^{\mu_1\dots\mu_n}(v;\alpha)\,, \\ \int \mathrm{d}^d s\, \frac{s^{\mu_1}\dots s^{\mu_n}}{(-s^2)^{\alpha}[-(s-q)^2]^{\beta}} &= i\pi^{d/2} G_n(\alpha,\beta)\,(-q^2)^{d/2-\alpha-\beta}\, J^{\mu_1\dots\mu_n}(q;\alpha,\beta)\,, \end{aligned} \tag{12}$$

with

$$I_n(\alpha,\beta) = \frac{\Gamma(d/2-\alpha+n)\,\Gamma(2\alpha+\beta-d-n)}{\Gamma(\alpha)\,\Gamma(\beta)}\,,$$

$$G_n(\alpha,\beta) = \frac{\Gamma(d/2-\alpha+n)\,\Gamma(d/2-\beta)\,\Gamma(\alpha+\beta-d/2)}{\Gamma(\alpha)\,\Gamma(\beta)\,\Gamma(d-\alpha-\beta+n)}\,. \tag{13}$$

The tensor structures are

$$K^{\mu_1\cdots\mu_n}(v;\alpha) = \sum_{j=0}^{[n/2]} (-1)^{n-j}\, C(n,j;\alpha) \sum_{\nu_i=\sigma(\mu_i)}{}' g^{\nu_1\nu_2}\ldots g^{\nu_{2j-1}\nu_{2j}}\, v^{\nu_{2j+1}}\ldots v^{\nu_n}\,,$$

$$J^{\mu_1\cdots\mu_n}(q;\alpha,\beta) = \sum_{j=0}^{[n/2]} (-q^2)^j\, D(n,j;\alpha,\beta) \sum_{\nu_i=\sigma(\mu_i)}{}' g^{\nu_1\nu_2}\ldots g^{\nu_{2j-1}\nu_{2j}}\, q^{\nu_{2j+1}}\ldots q^{\nu_n}\,, \tag{14}$$

where $[n/2]$ is the largest integer less than or equal to $n/2$, and

$$C(n,j;\alpha) = \prod_{k=1}^{j} \frac{1}{d+2(n-k-\alpha)}\,,$$

$$D(n,j;\alpha,\beta) = \prod_{k=1}^{j} \frac{d+2(k-1-\beta)}{[d+2(n-k-\alpha)][d+2(k-\alpha-\beta)]}\,. \tag{15}$$

The primed sums in (14) mean a summation over all $\binom{n}{2j}(2j-1)!!$ permutations that lead to a different assignment of indices.

Using this technique, we have calculated the pole parts of the two-loop diagrams shown in Fig. 2. We adopt the background-field formalism [17]–[19] and work in the 't Hooft–Feynman gauge. The final expression for the sum of all diagrams is gauge independent. The pole parts proportional to $v^\alpha v^\nu q^\mu$ are given in Tab. 1 for each diagram. Here $C_A = N$, $C_F = (N^2-1)/(2N)$, $T_F = 1/2$ are the colour factors for an $SU(N)$ gauge group, and $n_f$ is the number of light-quark flavours. The renormalization scale $\mu$ is introduced by the replacement of the bare coupling constant with the renormalized one through the relation $g_s^{\rm bare} = \bar\mu^\epsilon Z_g\, g_s$, with $\bar\mu = \mu\, e^{\gamma_E/2}(4\pi)^{-1/2}$ in the $\overline{\rm MS}$ scheme.

# 3 Ultraviolet Counterterms

The two-loop diagrams in Fig. 2 contain subdivergences, which must be subtracted by UV counterterms. We first discuss the one-loop counterterms for the heavy-quark and gluon propagators and vertices. The corresponding terms in the Lagrangian are

$$\begin{aligned}\mathcal{L}_{c.t.} = {}& \delta_h\,\bar h_v\, iv\cdot\partial\, h_v - \frac{\delta_A}{2}\,(\partial_\mu A^a_\nu - \partial_\nu A^a_\mu)\,\partial^\mu A^{\nu a} + \bar\mu^\epsilon g_s\,\delta_{hhA}\,\bar h_v\, v\cdot A\, h_v \\ & - \bar\mu^\epsilon g_s\,\delta_{BAA}\, f^{abc}\left[(\partial_\mu B^a_\nu)A^{\mu b}A^{\nu c} + (\partial_\mu A^a_\nu)B^{\mu b}A^{\nu c} + (\partial_\mu A^a_\nu)A^{\mu b}B^{\nu c}\right]\,,\end{aligned} \tag{16}$$

Table 1: Pole parts proportional to $g_s t_a \Gamma\, v^\alpha v^\nu q^\mu$ of the two-loop diagrams in units of $(\alpha_s/4\pi)^2$. The diagrams $D_6$, $D_8$, $D_{14}$, $D_{16}$, $D_{24}$ and $D_{25}$ vanish or do not yield the desired Lorentz structure.

| | colour factor | $\times \left(\frac{-2\omega}{\mu}\right)^{-4\epsilon}$ | $\times \left(\frac{-2\omega}{\mu}\right)^{-2\epsilon} \left(\frac{-q^2}{\mu^2}\right)^{-\epsilon}$ |
|---|---|---|---|
| $D_1$ | $C_A^2$ | $\frac{1}{16\epsilon}$ | |
| $D_2$ | $C_A^2$ | $-\frac{1}{8\epsilon^2} - \left(\frac{101}{48} - \frac{\pi^2}{9}\right)\frac{1}{\epsilon}$ | $\frac{1}{\epsilon^2} + \frac{6}{\epsilon}$ |
| $D_3$ | $C_A^2$ | $\left(\frac{1}{6} - \frac{\pi^2}{9}\right)\frac{1}{\epsilon}$ | |
| $D_4$ | $C_A^2$ | $-\frac{3}{4\epsilon^2} - \frac{9}{8\epsilon}$ | |
| $D_5$ | $C_A^2$ | $-\frac{1}{2\epsilon^2} - \frac{7}{8\epsilon}$ | $\frac{1}{\epsilon^2} + \frac{2}{\epsilon}$ |
| $D_7$ | $C_A^2$ | $\frac{11}{8\epsilon^2} + \left(\frac{85}{24} - \frac{\pi^2}{9}\right)\frac{1}{\epsilon}$ | $-\frac{1}{\epsilon^2} - \frac{6}{\epsilon}$ |
| $D_9$ | $C_A^2$ | $\left(\frac{1}{3} + \frac{\pi^2}{9}\right)\frac{1}{\epsilon}$ | |
| $D_{10}$ | $C_A(C_A - 2C_F)$ | $\frac{1}{2\epsilon^2} + \frac{1}{\epsilon}$ | |
| $D_{11}$ | $C_A(C_A - 2C_F)$ | $\frac{1}{2\epsilon^2} - \frac{1}{\epsilon}$ | |
| $D_{12}$ | $C_A(C_A - 2C_F)$ | $\frac{1}{2\epsilon^2} + \frac{1}{\epsilon}$ | |
| $D_{13}$ | $C_A^2$ | $\frac{1}{\epsilon^2} + \frac{2}{\epsilon}$ | $-\frac{2}{\epsilon^2} - \frac{8}{\epsilon}$ |
| $D_{15}$ | $C_A^2$ | $-\frac{2}{\epsilon^2} - \frac{4}{\epsilon}$ | $\frac{2}{\epsilon^2} + \frac{8}{\epsilon}$ |
| $D_{17}$ | $C_A C_F$ | $\frac{1}{\epsilon^2} + \frac{2}{\epsilon}$ | |
| $D_{18}$ | $C_A^2$ | $\frac{5}{24\epsilon^2} + \frac{49}{72\epsilon}$ | $\frac{1}{\epsilon^2} + \frac{5}{2\epsilon}$ |
| $D_{19}$ | $C_A T_F\, n_f$ | $\frac{2}{3\epsilon^2} - \frac{5}{9\epsilon}$ | |
| $D_{20}$ | $C_A^2$ | $-\frac{1}{24\epsilon^2} - \frac{5}{72\epsilon}$ | |
| $D_{21}$ | $C_A^2$ | | $-\frac{3}{\epsilon^2} - \frac{6}{\epsilon}$ |
| $D_{22}$ | $C_A^2$ | $-\frac{9}{16\epsilon^2} - \frac{9}{32\epsilon}$ | |
| $D_{23}$ | $C_A^2$ | $\frac{9}{16\epsilon^2} + \frac{9}{32\epsilon}$ | |
| $D_{26}$ | $C_A^2$ | $\frac{5}{6\epsilon^2} + \frac{17}{36\epsilon}$ | |
| | $C_A T_F\, n_f$ | $-\frac{2}{3\epsilon^2} - \frac{1}{9\epsilon}$ | |
| $D_{27}$ | $C_A^2$ | $\frac{5}{6\epsilon^2} + \frac{47}{36\epsilon}$ | |
| | $C_A T_F\, n_f$ | $-\frac{2}{3\epsilon^2} - \frac{7}{9\epsilon}$ | |
| Sum | $C_A^2$ | $\frac{7}{3\epsilon^2} + \frac{25}{18\epsilon}$ | $-\frac{1}{\epsilon^2} - \frac{3}{2\epsilon}$ |
| | $C_A C_F$ | $-\frac{2}{\epsilon^2}$ | |
| | $C_A T_F\, n_f$ | $-\frac{2}{3\epsilon^2} - \frac{13}{9\epsilon}$ | |

where $A^\mu$ is the conventional gluon field, and $B^\mu$ the background field. In the Feynman gauge, the counterterm coefficients are

$$\begin{aligned}
\delta_h &= Z_h - 1 = 2C_F\,\frac{\alpha_s}{4\pi\epsilon}\,, \\
\delta_A &= Z_A - 1 = \left(\frac{5}{3}\,C_A - \frac{4}{3}\,T_F\,n_f\right)\frac{\alpha_s}{4\pi\epsilon}\,, \\
\delta_{hhA} &= Z_g Z_h Z_A^{1/2} - 1 = (-C_A + 2C_F)\,\frac{\alpha_s}{4\pi\epsilon}\,, \\
\delta_{BAA} &= Z_g Z_B^{1/2} Z_A - 1 = \delta_A\,,
\end{aligned} \tag{17}$$

where $Z_A$ is the wave-function renormalization factor for the gluon field, and $Z_B^{1/2} = Z_g^{-1}$ holds for the background field [19]. Note that the Feynman rule for the counterterm for the three-gluon vertex with a background field is the same as that for the usual three-gluon vertex, but with a different renormalization factor.

In addition, the two-loop diagrams in Fig. 2 contain subdivergences that are removed by operator counterterms. To find these counterterms, we calculate at the one-loop order all insertions of the operator $O_1^{\mu\nu}$ into the amputated Green functions with a non-negative degree of divergence. They have the field content $\bar h_v h_v$, $\bar h_v h_v A$, $\bar h_v h_v B$, $\bar h_v h_v AA$, $\bar h_v h_v AB$, $\bar h_v h_v BB$ and $\bar h_v h_v \eta\bar\eta$, where $\eta$ is a ghost field. It turns out that there are no UV divergences in the Green function containing ghost fields, and that the insertion of $O_1^{\mu\nu}$ into the heavy-quark two-point function vanishes. The remaining divergences can be removed by adding counterterms proportional to the original operators $O_1^{\mu\nu}$ and $O_2^{\mu\nu}$ in (3), as well as to the operators

$$\begin{aligned}
O_3^{\mu\nu} &= \bar h_v \Gamma\,(v^\mu Q^\nu - v^\nu Q^\mu)\,iv\cdot D\,h_v \\
&\quad + \bar h_v\,(iv\cdot \overleftarrow{D}^\dagger)\,\Gamma\,(v^\mu Q^\nu - v^\nu Q^\mu)\,h_v\,, \\
O_4^{\mu\nu} &= \bar h_v \Gamma\,([iD^\mu, Q^\nu] - [iD^\nu, Q^\mu])\,h_v\,, \\
O_5^{\mu\nu} &= v^\mu v_\rho O_4^{\rho\nu} - v^\nu v_\rho O_4^{\rho\mu}\,, \\
O_6^{\mu\nu} &= \bar h_v \Gamma\,[Q^\mu, Q^\nu]\,h_v\,, \\
O_7^{\mu\nu} &= v^\mu v_\rho O_6^{\rho\nu} - v^\nu v_\rho O_6^{\rho\mu}\,.
\end{aligned} \tag{18}$$

Here $Q^\mu$ is the 'quantum part' of the gluon field, defined by the decomposition $A^\mu = B^\mu + Q^\mu$. Under a local gauge transformation, the background and the quantum field transform as

$$\begin{aligned}
B^\mu(x) &\to U(x)\,B^\mu(x)\,U^\dagger(x) + \frac{i}{g_s}\,[\partial^\mu U(x)]\,U^\dagger(x)\,, \\
Q^\mu(x) &\to U(x)\,Q^\mu(x)\,U^\dagger(x)\,,
\end{aligned} \tag{19}$$

with $U(x) \in SU(N)$, so that the gluon field $A^\mu$ obeys the usual transformation law. The operators containing the quantum part of the gluon field are needed as insertions inside

Table 2: Pole parts proportional to $g_s t_a \Gamma\, v^\alpha v^\nu q^\mu$ of the one-loop diagrams with counterterm insertions in units of $(\alpha_s/4\pi)^2$. The diagram $C_8$ does not contribute.

| | colour factor | $\times \left(\frac{-2\omega}{\mu}\right)^{-2\epsilon}$ | $\times \left(\frac{-q^2}{\mu^2}\right)^{-\epsilon}$ |
|---|---|---|---|
| $C_1$ | $C_A C_F$ | $-\frac{2}{\epsilon^2}$ | |
| $C_2$ | $C_A^2$ | $-\frac{5}{3\epsilon^2}$ | |
| | $C_A T_F\, n_f$ | $\frac{4}{3\epsilon^2}$ | |
| $C_3$ | $C_A^2$ | $-\frac{5}{3\epsilon^2}$ | |
| | $C_A T_F\, n_f$ | $\frac{4}{3\epsilon^2}$ | |
| $C_4$ | $C_A^2$ | $\frac{5}{3\epsilon^2}$ | |
| | $C_A T_F\, n_f$ | $-\frac{4}{3\epsilon^2}$ | |
| $C_5$ | $C_A(C_A - 2C_F)$ | $-\frac{1}{\epsilon^2}$ | |
| $C_6$ | $C_A(C_A - 2C_F)$ | $-\frac{1}{\epsilon^2}$ | |
| $C_7$ | $C_A C_F$ | $\frac{2}{\epsilon^2}$ | |
| $C_9$ | $C_A^2$ | | $\frac{1}{\epsilon^2} + \frac{2}{\epsilon}$ |
| Sum | $C_A^2$ | $-\frac{11}{3\epsilon^2}$ | $\frac{1}{\epsilon^2} + \frac{2}{\epsilon}$ |
| | $C_A C_F$ | $\frac{4}{\epsilon^2}$ | |
| | $C_A T_F\, n_f$ | $\frac{4}{3\epsilon^2}$ | |

loop diagrams. Since the quantum field $Q^\mu$ transforms in the same way as the covariant derivative, they are all gauge invariant. The (class-2) operator $O_3^{\mu\nu}$, which vanishes by the equations of motion, has to be included since the two-loop calculation is performed off-shell. The one-loop counterterm coefficients $\delta_n$ are

$$\delta_1 = (C_A + 2C_F)\,\frac{\alpha_s}{4\pi\epsilon}\,, \qquad \delta_2 = 2\delta_3 = \delta_4 = -C_A\,\frac{\alpha_s}{4\pi\epsilon}\,, \tag{20}$$

and $\delta_5 = \delta_7 = 0$. The coefficient $\delta_6$ is irrelevant for our purposes, since insertions of the operator $O_6^{\mu\nu}$ into one-loop diagrams do not contribute to the Lorentz structure $v^\alpha v^\nu q^\mu$.

The one-loop diagrams with counterterm insertions, which are required to cancel the subdivergences of the two-loop diagrams in Fig. 2, are shown in Fig. 4. The resulting pole parts are listed in Tab. 2. Note that most of the counterterm contributions are pure $1/\epsilon^2$ poles, since the original diagrams in Fig. 1 do not have $O(\epsilon^0)$ terms. When the counterterm contributions are added to the results for the two-loop diagrams, all non-local $1/\epsilon$ divergences proportional to $\ln(-2\omega/\mu)$ and $\ln(-q^2/\mu^2)$ cancel. This is a strong check of our calculation. For the coefficient of $(\alpha_s/4\pi)^2$, indicated by the subscript in

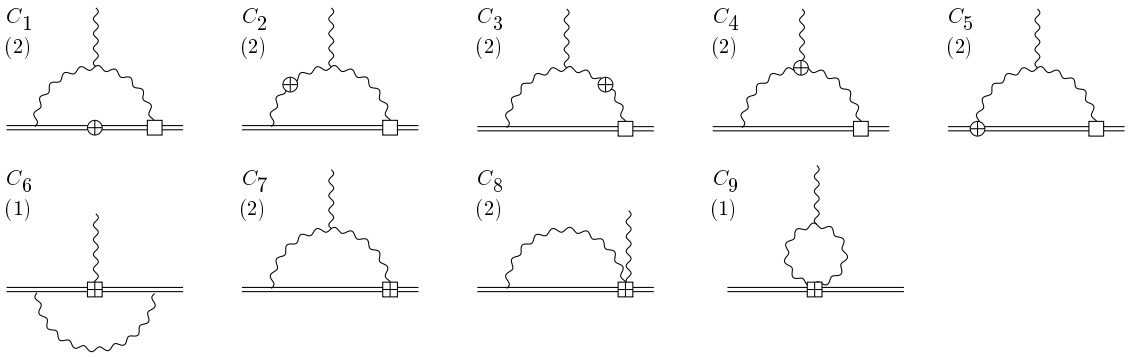


Figure 4: Counterterm insertion diagrams contributing to the calculation of the renormalization factor $Z_2$.

square brackets, times the tree-level matrix element of $O_2^{\mu\nu}$, we obtain

$$-\left(Z_h Z_2\right)_{[2]} = C_A^2 \left(-\frac{4}{3\epsilon^2} + \frac{17}{9\epsilon}\right) + C_A C_F \, \frac{2}{\epsilon^2} + C_A T_F \, n_f \left(\frac{2}{3\epsilon^2} - \frac{13}{9\epsilon}\right) . \tag{21}$$

To obtain $Z_2$, we have to account for the wave-function renormalization of the heavy-quark fields. (There is no renormalization of the background field, since $Z_g Z_B^{1/2}$ [19].) This removes the $C_A C_F$ term. Using then relation (5) leads to

$$Z_{\rm mag} = 1 + \frac{C_A \alpha_s}{4\pi\epsilon} + \left(\frac{\alpha_s}{4\pi}\right)^2 \left[ \left(-\frac{4}{3}\, C_A^2 + \frac{2}{3}\, C_A T_F \, n_f\right) \frac{1}{\epsilon^2} + \left(\frac{17}{9}\, C_A^2 - \frac{13}{9}\, C_A T_F \, n_f\right) \frac{1}{\epsilon} \right] . \tag{22}$$

The coefficient of the $1/\epsilon^2$ pole in $Z_{\rm mag}$ obeys the relation

$$Z^{(2)}_{\rm mag,[2]} = \frac{1}{2}\, Z^{(1)}_{\rm mag,[1]} \left(Z^{(1)}_{\rm mag,[1]} - \beta_0\right) , \tag{23}$$

where $\beta_0$ is the first coefficient of the $\beta$ function (see (26) below), and the super- and subscripts in round (square) brackets have the same meaning as before. Eq. (23) is a necessary condition for $\gamma_{\rm mag}$ to be finite as $\epsilon \to 0$ [9]. For the anomalous dimension of the chromo-magnetic operator in the $\overline{\rm MS}$ scheme, we now obtain from (2)

$$\gamma_{\rm mag} = \frac{C_A \alpha_s}{2\pi} \left[1 + \left(\frac{17}{18}\, C_A - \frac{13}{18}\, T_F \, n_f\right) \frac{\alpha_s}{\pi} + O(\alpha_s^2)\right] . \tag{24}$$

This is our main result.

# 4 Conclusions

Using a relation between renormalization constants that is a consequence of the re-parametrization invariance and the virial theorem, we have found an efficient way to calculate the two-loop anomalous dimension of the chromo-magnetic operator in the

HQET. The calculation involves the evaluation of 25 non-vanishing two-loop diagrams. Some of these diagrams have IR divergences that must be regulated by keeping the external gluon off-shell. After these divergences are subtracted using a simple variant of the $R^*$ operation, the external momentum can be set to zero and the resulting two-loop propagator-type tensor integrals can be evaluated using a recurrence relation, which allows to express them in terms of products of one-loop integrals.

Our result for the anomalous dimension in (24) is rather simple. In our approach, it is obvious from the beginning that the 'abelian' colour structures $C_F^2$ and $C_F T_F\, n_f$ do not appear; because of the selection rules given in section 2, the result for the anomalous dimension is genuinely non-abelian, proportional to $C_A$. This would not be obvious if the calculation were performed in the standard way by studying the mixing of the chromo-magnetic operator with itself. More surprisingly, there is no contribution proportional to $C_A C_F$ in the final result, and also all terms proportional to $\pi^2$ have disappeared. This is in contrast with the two-loop anomalous dimension of current operators, where such terms do appear [15, 20]–[22].

If, instead of an $SU(N)$ gauge theory, we consider the abelian $U(1)$ gauge theory, the right-hand side of (24) vanishes, since then $C_A = 0$ (and $C_F = T_F = 1$). In our approach, it is easy to see that in the abelian theory the anomalous dimension of the magnetic-moment operator actually vanishes to all orders in perturbation theory. According to the selection rules, in the absence of gauge-boson self-couplings the external photon can be connected to the operator and the heavy-quark lines only through a fermion loop with at least four photons attached. Such a diagram is convergent except for subgraphs that correspond to charge and field renormalization. Consequently, no operator counterterms are needed.

With our two-loop result for $\gamma_{\rm mag}$ at hand, we can evaluate the Wilson coefficient of the chromo-magnetic operator in the effective Lagrangian (1) to next-to-leading order. The result is

$$C_{\rm mag}(m_Q/\mu) = \left(\frac{\alpha_s(m_Q)}{\alpha_s(\mu)}\right)^{\gamma_0/2\beta_0} \left[1 + \frac{\alpha_s(m_Q)}{4\pi}\, c_1 + \frac{\alpha_s(m_Q) - \alpha_s(\mu)}{4\pi} \left(\frac{\gamma_1}{2\beta_0} - \frac{\gamma_0\beta_1}{2\beta_0^2}\right) + \ldots\right] \tag{25}$$

where $c_1 = 2(C_A + C_F)$ is obtained from one-loop matching [3]. The one- and two-loop coefficients of the anomalous dimension and $\beta$ function are

$$\begin{aligned}
\gamma_0 &= 2C_A\,, \qquad \gamma_1 = \frac{68}{9}\, C_A^2 - \frac{52}{9}\, C_A T_F\, n_f\,, \\
\beta_0 &= \frac{11}{3}\, C_A - \frac{4}{3}\, T_F\, n_f\,, \\
\beta_1 &= \frac{34}{3}\, C_A^2 - \frac{20}{3}\, C_A T_F\, n_f - 4 C_F T_F\, n_f\,.
\end{aligned} \tag{26}$$

As an application, we discuss the mass splitting between the ground-state vector and pseudoscalar mesons containing a bottom or a charm quark. To leading order in the

heavy-quark expansion, one finds [1]

$$R \equiv \frac{m_{B^*}^2 - m_B^2}{m_{D^*}^2 - m_D^2} = \frac{C_{\rm mag}(m_b/\mu)}{C_{\rm mag}(m_c/\mu)} + O(1/m_Q)\,. \tag{27}$$

For $N = 3$ colours and $n_f = 4$ light-quark flavours (as it is appropriate in the region between the bottom- and charm-quark masses)

$$R = \left(\frac{\alpha_s(m_b)}{\alpha_s(m_c)}\right)^{9/25} \left[1 - \frac{7921}{3750}\,\frac{\alpha_s(m_c) - \alpha_s(m_b)}{\pi}\right] + \Lambda_R \left(\frac{1}{m_c} - \frac{1}{m_b}\right)\,, \tag{28}$$

where the non-perturbative parameter $\Lambda_R$ accounts for higher-order corrections in the heavy-quark expansion. Using $\alpha_s(m_b) = 0.22$ and $\alpha_s(m_c) = 0.36$, we obtain $R \approx 0.76$, in reasonable agreement with the experimental value $R_{\rm exp} = 0.89 \pm 0.01$. The next-to-leading correction in (28) amounts to minus 10% and deteriorates the comparison with the experimental value. However, with $\Lambda_R \approx 200\,\text{MeV}$ required for agreement with $R_{\rm exp}$, higher-order corrections in the $1/m_Q$ expansion remain moderate in size.

*Acknowledgements:* We are indebted to A. Grozin for communicating partial results of an independent calculation of $\gamma_{\rm mag}$ based on a different technique. One of us (M.N.) would like to thank M. Ciuchini, J. Körner and D. Kreimer for useful discussions. G.A. acknowledges a grant from the Generalitat Valenciana, and partial support by DGICYT under grant PB94-0080. He also acknowledges the hospitality of the CERN Theory Division, where this research was performed.

# References

[1] For a review, see: M. Neubert, Phys. Rep. **245**, 259 (1994); Int. J. Mod. Phys. **A11**, 4173 (1996).

[2] H. Georgi, Phys. Lett. **B240**, 447 (1990).

[3] E. Eichten and B. Hill, Phys. Lett. **B243**, 427 (1990).

[4] A.F. Falk, B. Grinstein and M.E. Luke, Nucl. Phys. **B357**, 185 (1991).

[5] M. Luke and A.V. Manohar, Phys. Lett. **B286**, 348 (1992).

[6] L. Maiani, G. Martinelli and C.T. Sachrajda, Nucl. Phys. **B368**, 281 (1992); G. Martinelli and C.T. Sachrajda, Phys. Lett. **B354**, 423 (1995); Nucl. Phys. **B478**, 660 (1996).

[7] M. Neubert, CERN preprint CERN-TH/96-282 (1996) [hep-ph/9610471], to appear in Phys. Lett. **B**.

[8] W.A. Bardeen, A.J. Buras, D.W. Duke and T. Muta, Phys. Rev. **D18**, 3998 (1978).

[9] E.G. Floratos, D.A. Ross and C.T. Sachrajda, Nucl. Phys. **B129**, 66 (1977).

[10] M. Misiak and M. Münz, Phys. Lett. **B344**, 308 (1995).

[11] G. Amorós and M. Neubert, CERN preprint CERN-TH/96-336 (1996) [hep-ph/9612298], to appear in Phys. Lett. **B**. Note that our definition of the renormalization factors differs from the one used in this reference.

[12] M. Neubert, Phys. Lett. **B322**, 419 (1994).

[13] A.A. Vladimirov, Teor. Mat. Phys. **43**, 210 (1980).

[14] K.G. Chetyrkin and F.V. Tkachov, Phys. Lett. **B114**, 340 (1982); K.G. Chetyrkin and V.A. Smirnov, Phys. Lett. **B144**, 419 (1984).

[15] D.J. Broadhurst and A.G. Grozin, Phys. Lett. **B267**, 105 (1991).

[16] K.G. Chetyrkin and F.V. Tkachov, Nucl. Phys. **B192**, 159 (1981).

[17] G. 't Hooft, in: Functional and Probabilistic Methods in Quantum Field Theory, Proc. XII Winter School of Theoretical Physics, Karpacz 1975, Acta Univ. Wratisl. **368**, 345 (1976).

[18] D. Boulware, Phys. Rev. **D23**, 389 (1981).

[19] L.F. Abbott, Nucl. Phys. **B185**, 189 (1981); Acta Phys. Pol. **C13**, 33 (1982).

[20] X. Ji and M.J. Musolf, Phys. Lett. **B257**, 409 (1991).

[21] G.P. Korchemsky and A.V. Radyushkin, Nucl. Phys. **B283**, 342 (1987); Phys. Lett. **B279**, 359 (1992); G.P. Korchemsky, Mod. Phys. Lett. **A4**, 1257 (1989).

[22] W. Kilian, P. Manakos and T. Mannel, Phys. Rev. **D48**, 1321 (1993).